

Seismic anisotropy and vertical fractures in the Edwards aquifer

Robert J. Ferguson, Department of Geological Sciences, University of Texas at Austin

SUMMARY

High resolution seismic data are acquired from the Edwards limestone formation in an area of outcrop within the Government Canyon State Natural Area, to infer the local orientation of vertical fracturing. The experiment consists of a single 3D seismic array of 16 3C recording stations. Seismic sources are deployed in and around the array at short spacings resulting in 16 3C source gathers (by reciprocity) with thousands of traces. A velocity-variation-with-azimuth trend is discernible in the data attributable to azimuthal anisotropy due to vertical fracturing. A slow direction along 120 degrees from North is found, with a fast direction along 20 degrees from North. If vertical fracturing and seismic anisotropy are correlated at this site, a fracture orientation along 20 degrees from North is determined.

INTRODUCTION

The hydraulic permeability of fractured aquifers and karstic aquifers is, in general, anisotropic (Palmer, 1999; Arnow, 1963), and in a fractured karstic aquifer like the Edwards formation, anisotropic permeability is thought to be dominated by fractures (Halihan et al., 2000). Seismic velocity in fractured media is similarly dominated by fracturing and, for a given fracture orientation, a fast direction along the cracks and a slow direction normal to the cracks is often apparent (Eshelby, 1957; Rathore et al., 1994). Critical to understanding how fracturing in solid rock affects both permeability and seismic velocity is the concept of anisotropy.

Anisotropy is a descriptive term for the observation that, in an experiment, the data obtained in an otherwise homogeneous medium change depending on the spatial orientation of the recording system. For hydraulic permeability, this can mean that the direction of water flow indicated by water levels in wells differs from the actual flow (Figure 1a), or when a well is pumped, an elongate cone of depression is observed where the long axis is along the dominant fracture direction (Figure 1b). For seismic wave propagation, fracture anisotropy can be seen in traveltimes isochrons that are not symmetric (Figure 2).

Seismic anisotropy associated with tectonic stress is most often due to regional the alignment of regional extension cracks (Thomsen, 2002). In the Edwards formation, fracturing is due to the tectonism associated with the Balcones Fault, and analysis of outcrops suggests that fractures are generally trending NE-SW.

Recognizing that hydraulic anisotropy and seismic anisotropy may be correlated in the Edwards formation, a seismic survey was acquired to establish whether the seismic method is useful for determining fracture orientation. The survey consists of 16 multi-component seismometers and 128 source locations centered on the Little Windmill well. The seismometers are situated in an $18m \times 18m$ grid, and the sources occupy an approximately square $60m \times 60m$ grid.

The Government Canyon State Natural Area (GCSNA) was chosen as a good test site for the following reasons:

1. The Edwards formation outcrops at GCSNA
2. Including Little Windmill, two well locations are available with fairly deep wells $\sim 165ft$ and access is good for future geophysical logging
3. The GCSNA staff strongly support use of the area for studies that will help protect the area

First break analysis of the recorded data is used to estimate the apparent velocity for the formation at the survey location. Due to the

Recorder	2 \times Geometrics Inc. GEODE
Channels	48
Sample rate	0.25 ms
Record length	0.5 s
Field filters	out
Source	Weight drop
Stacks per record	3
Geophones	16 \times Geometrics Inc. 3C geophones
Natural freq.	10 Hz V, 8Hz H
Power	2 \times 12 V batt.
Emergency power	Honda EU 2000W

Table 1: Description of recorder, source, 3C geophones, and power supply. This highly portable system was assembled to comply with the noise and vehicular traffic restrictions in the Government Canyon State Natural Area, yet still achieve high-quality data.

very low apparent velocity ($500 \frac{m}{s} < v < 1500 \frac{m}{s}$), surface waves are assumed to be represented in the interpreted first breaks, and the body waves (the actual first breaks) lie to low in the noise to be analyzed (Beatty and Schmitt, 2003). Apparent velocity is then averaged along different azimuthal trajectories and a curve of average apparent velocity verses azimuth is plotted.

The goal of this study is acquire data to help to identify a correlation between fractures in the Edwards formation and seismic anisotropy. If a correlation can be made, then regional estimates of the dominant direction of fracture permeability can be made using the non-destructive, non-invasive technology of 3D seismic, and will assist in urban planning, and estimation of contaminant flow.

DATA ACQUISITION AND PROCESSING

As Government Canyon State Natural Area is a protected area, vehicular traffic is restricted, and noise, and brush removal are prohibited. At the Little Wind Mill well site, the closest vehicular access is $\sim 2km$ away, so a quiet, highly portable acquisition system was assembled and deployed. The acquisition system and power supply are summarized in Table 1.

Processing goals consist of careful merging of survey data and traces to ensure accurate source-receiver offsets, and enhancement of first arrivals to ensure accurate travel-time picking.

Acquisition

The Edwards formation outcrops everywhere at the Little Wind Mill well site, and the source receiver offsets are $< 60m$, so a light, low energy source is used.

The 3C geophones are pictured in Figure 3. Where surface cover is available, a standard geophone plant provides good coupling. Where solid limestone is encountered, a block of modeler's clay is used as a base for the geophone (Figure 3 right side). (The clay is in a plastic bag to slow hardening and facilitate removal from the site).

Total weight of the system, including the total station survey instrument and survey rods is about 500 lb, and it all fits easily into a 3/4 ton pickup.

No vegetation can be disturbed at GCSNA and this is reflected in the irregularity of the source and receiver locations (Figure 4). The grid spacing is a nominal $6 \times 6m$, but thorny vegetation in the upper left quadrant (Figure 4) prevents access to that area. Two base stations

were required to complete the survey due to restricted lines of site. A potential source of error was the use of a very long survey rod to see over thick bushes (true vertical positioning of the rod was difficult).

A total of 5888 traces were acquired from 128 source locations and 46 channels (two channels - one vertical, and one horizontal, were open circuits). At source stations where Edwards outcrops, the source would bounce causing a secondary source. This source of seismic noise was mitigated by having the field assistant catch and hold the weight after the initial impact.

The quality of recorded body-waves suffers from the dominance of surface wave energy as can be seen in Figures 5, 6, and 7.

First-arrival analysis (described in detail below) resolves apparent velocities for offsets $\leq 12m$ of $\sim 500 \frac{m}{s}$, with velocity increasing to $\sim 1500 \frac{m}{s}$ at far offsets $\sim 60m$. As the P-wave velocity of limestone is not expected to vary significantly with offset, and be much higher ($3400 - 6000 \frac{m}{s}$), identification of surface as the first interpretable arrivals is verified.

Processing

To ensure accurate picking of first arriving surface waves, seismic noise including low-energy body-waves must be removed, and first arrivals must be enhanced with respect to later arrivals. To this end, the following processing flow was used:

1. Merge surveys from the two base stations using a least-squares rotation/translation operator (based on two stations surveyed from each base station)
2. Reduce noise (including body waves) in advance of the first arrivals by computing the magnitude (the magnitude of all three receiver elements for each receiver station)
3. Apply a 21 point median filter to further enhance the first arrival
4. Differentiate and compute the absolute value
5. Sort into common offset and establish a first break window for each offset (6m bins)
6. Pick the traveltimes to the largest absolute value within the first-break window

An example of a common receiver gather sorted by source number is given in Figure 8. Of course, automatic picking by the above method saves time in processing at the expense of pick quality.

Picks are interpolated to an even .5m spacing using cubic splines. For each trace, division of offset by picktime results in an apparent velocity. Plan-views of the apparent velocity data for four receiver stations are given in Figure 9.

Contours close to the source point are $\sim 500 \frac{m}{s}$ and increase to $\sim 1500 \frac{m}{s}$ at the edges of the survey. Obvious variation in apparent velocity with azimuth is not apparent in the contour data so curves of average apparent-velocity versus azimuth are computed in the following way: For each receiver location

1. Compute the maximum offset to the edge of the survey for compass directions 0 through 180 degrees
2. Define an offset window as the minimum of the above offsets as in Figure 10 (this ensures an even distribution of offsets for all azimuths)

3. Rotate the matrix of apparent velocities in 10 degree increments and compute the mean velocity for all points between the receiver location and the end of the offset window (for each azimuth, find the average velocity between the receiver location and the end of the arrow in Figure 10)

(Due to the missing upper quadrant, only the lower half of the survey was used to compute average apparent velocity versus azimuth.) The resultant average-apparent-velocity-verses-azimuth curves for each receiver station (Figure 11a) are summed into a single velocity-verses-azimuth curve (Figure 11b).

DISCUSSION AND CONCLUSIONS

If noise in the picktimes and survey data, and systematic errors have stacked out through the processing flows described above, a velocity variation with azimuth trend is discernible in Figure 11b. A slow direction is associated with approximately 120 degrees from North, and a fast direction is found 90 degrees from the slow direction at approximately 20 degrees from North.

At little windmill, if fractures and seismic anisotropy are correlated, a fracture orientation along 20 degrees from North is determined from this study. Further investigation is required to establish conclusively whether a fracture set is causing the apparent velocity anisotropy. Camera logging of the Little Windmill well may provide the local fracture orientation if the well intersects the fractures and if the highly oblique fracture traces can be interpreted. Further processing of the data to separate body waves from the dominant surface waves is necessary for imaging and shear-wave birefringence analysis that can further constrain a local fracture orientation.

ACKNOWLEDGMENTS

I wish to thank undergraduate Hunter Danke for assisting with this survey, and I wish to thank the Geology Foundation and EDGER Forum at the Jackson School of Geosciences, University of Texas at Austin for financial support. Special thanks to Erik R. Holmback and Deirdre E. Hisler of the Government Canyon State Natural Area for providing site access and field support.

REFERENCES

- Arnou, T., 1963, Ground water geology of bexar county: U.S. Geol. Survey.
- Beatty, K., and Schmitt, D., 2003, Repeatability of multi-mode rayleigh wave dispersion studies: *Geophysics*, **68**, no. 03, 782–790.
- Davis, S. N., and DeWeist, R. J. M., 1966, *Hydrogeology*: New York, John Wiley & Sons.
- Eshelby, J. D., 1957, The determination of elastic field of an ellipsoidal inclusion, and related problems: *Proc. R. Soc.*, pages 376 – 396.
- Halihan, T., Mace, R. E., and Sharp, J. M. F., 2000, Flow in the san antonio segment of the edwards aquifer: matrix, fractures, or conduits?: Rotterdam, A. A. Balkema.
- Palmer, A. N., 1999, *Anisotropy in carbonate aquifers*., 5 Karst Waters Institute.
- Rathore, J. S., Fjaer, E., Holt, R. M., and Renlie, L., 1994, Acoustic anisotropy of a synthetic sandstone with a controlled crack geometry: *Geophys. Prosp.*, **43**, 711–728.
- Thomsen, L., 2002, Understanding seismic anisotropy in exploration and exploitation: *Soc. of Expl. Geophys., Eur. Assn. Geosci. Eng.*

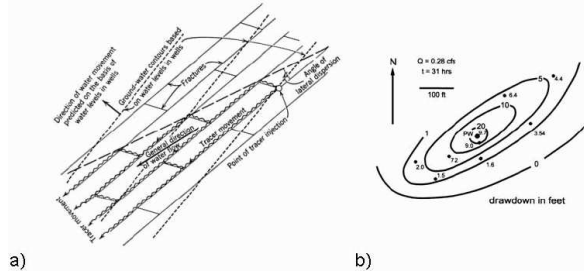


Figure 1: Hydraulic anisotropy and fluid flow. a) In a fractured formation, the direction of flow indicated by water levels measured in wells is different than the actual flow direction (adapted from (Davis and DeWeist, 1966)). b) An elongate cone of depressions results when a well is pumped. The long axis corresponds to the dominant fracture direction (from(Palmer, 1999)).

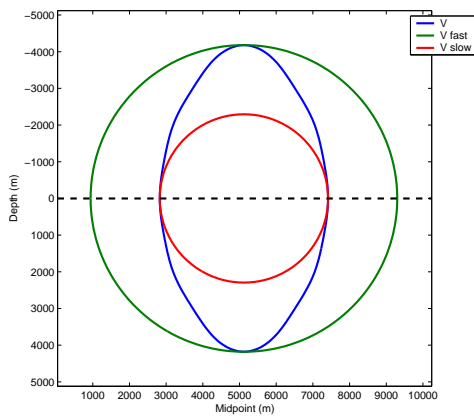


Figure 2: Travel time isochrons in a homogeneous medium with vertical fractures. In this example, a seismic wave propagating from the source location (5000,0) for a fixed amount of time travels farther in the vertical direction (along the fractures) than it does in the horizontal direction (across the fractures); the seismic velocity has a *fast* and a *slow* direction.



Figure 3: 3C geophones. Geophone coupling to hard surfaces like the Edwards limestone is a concern with spiked geophones. As a solution, when solid limestone is encountered, a block of modeler's clay is used as a base.

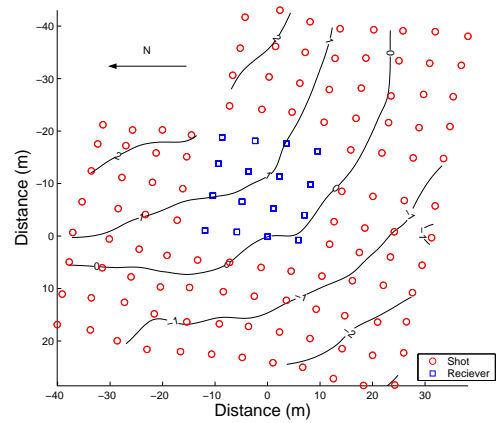


Figure 4: Plan view of survey layout with elevation contours. Nominal shot and receiver spacing is $6\text{m} \times 6\text{m}$. Access to the upper quadrant was prevented by dense, thorny vegetation.

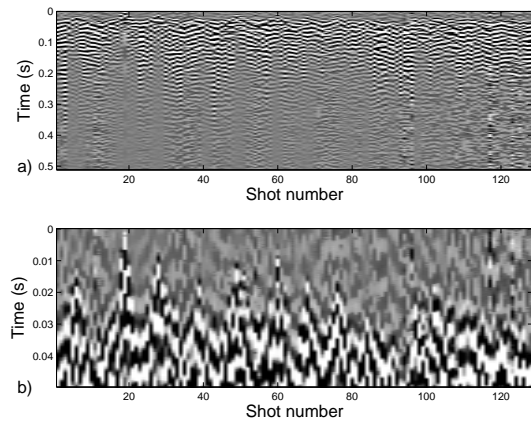


Figure 5: Common receiver gather. a) Unprocessed vertical component. b) Zoom of first breaks.

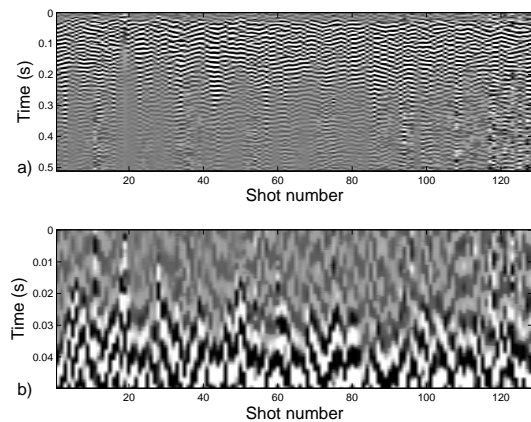


Figure 6: Common receiver gather. a) Unprocessed horizontal 1 component. b) Zoom of first breaks.

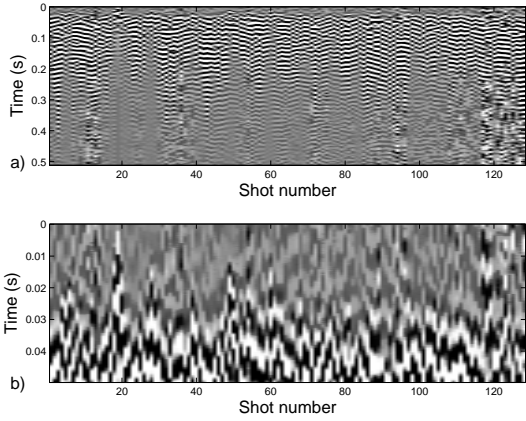


Figure 7: Common receiver gather. a) Unprocessed horizontal 2 components. b) Zoom of first breaks.

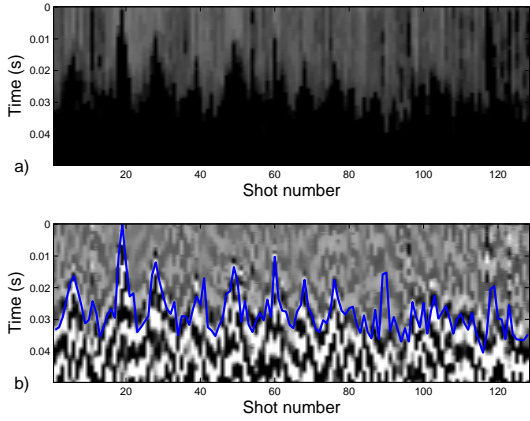


Figure 8: Common receiver gather with picks. a) Trace magnitude used for picking first breaks. A 21 point median filter is applied to sharpen the first break. b) Trace gather with picks. The quality of picks is generally good with a few exceptions, for example, at shot number 90. There, the pick is ~ 15 ms where it should be ~ 35 ms.

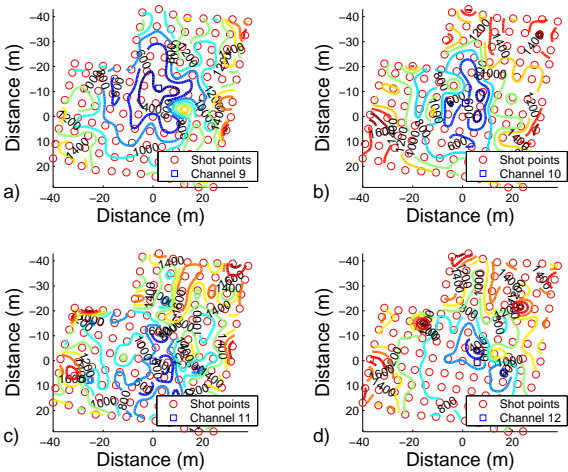


Figure 9: Plan view of apparent velocity for each receiver station a) station 9, b) station 10, c) station 11, d) station 12. Low velocity is centered on the receiver stations increasing with offset as deeper/faster parts of the formation are encountered.

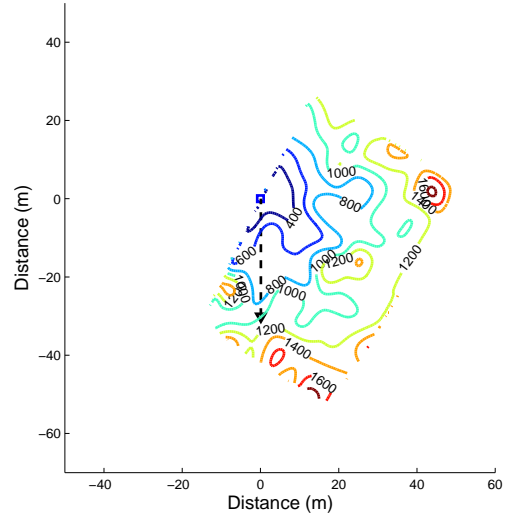


Figure 10: Average apparent velocity as a function of azimuth computed along the azimuth between the receiver location and a fixed offset. Only the lower half of the survey is analyzed to ensure equal representation of offsets within the analysis distance.

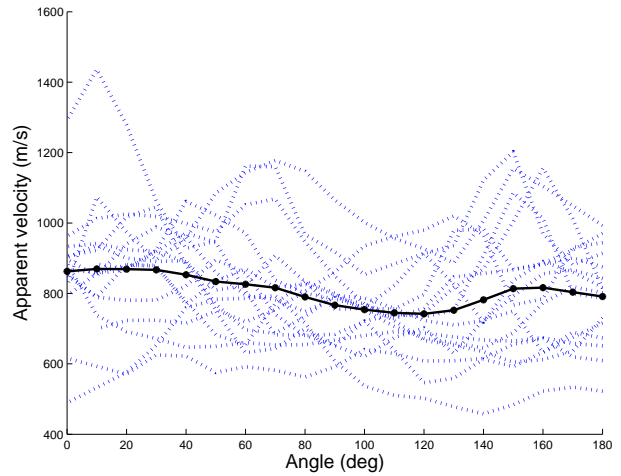


Figure 11: Average apparent velocity versus azimuth. a) Curves for all 16 stations. b) Mean of the curves in a). Assuming that pick errors and velocity heterogeneity average out, velocity is a minimum at approximately 120 degrees, and a maximum found at approximately 20 degrees. If seismic anisotropy and vertical fracturing are correlated at the Little Wind Mill wellsite, the fracture orientation of the Edwards formation is approximately 20 degrees from North.